Indian J. Phys. 76B (2), 177–183 (2002)

I J P B
an international journal

Measurement of L X-ray intensity ratios in Ta, W, Au, Hg, Pb and Bi using 2 MeV protons

Y Ramakrishna, K Ramachandra Rao, G J Naga Raju, P Venkateswarlu, K Bhaskara Rao, V Seshagiri Rao, M Ravi Kumar and S Bhuloka Reddy*

Swami Jnanananda Laboratories for Nuclear Research, Andhra University, Visakhapatnam-530 003, Andhra Pradesh, India

E-mail : sbr_r@yahoo.com

Received 10 August 2001, accepted 30 October 2001

Abstract : The L sub-shell intensity ratios, L_α/L_l, L_α/L_β and L_α/L_γ are measured in elements Ta, W, Au, Hg, Pb and Bi using 2 MeV proton projectiles. With the theoretical L sub-shell ionization cross section values of RPWBA and ECPSSR theories for 2 MeV protons and employing different sets of experimental data for fluorescence yields, C-K transitions yields, the L_α/L_l, L_α/L_β and L_α/L_γ intensity ratios are estimated. The present experimental values are compared with the theoretical intensity ratios thus obtained. Considering the errors in both experimental and theoretical intensity ratios, the present experimental ratios agree reasonably with the theoretical predictions based on the above two theoretical approaches with combinations of different available data bases.

Keywords : L X-ray intensity ratios 2 MeV proton beam-Si(Li) detector, ECPSSR and RPWBA theoretical predictions.

PACS Nos. : 32.80 Hd, 32.30.Rj, 41 75.Ak

1. Introduction

The study of inner-shell ionization process by charged particle bombardment is of importance to understand the mechanism involved in ion-atom interaction process. The present knowledge reveals that inner-shell ionization by charged particle takes place by two processes : direct ionization process and electron capture process. These two processes are appropriate for certain range of the parameters Z_1/Z_2 and V_1/V_2 where Z_1 and Z_2 are the projectile and target nuclear charges and V_1 and V_2 are the projectile velocity and mean velocity of the target electrons respectively. For $Z_1/Z_2 < 1$ and $V_1/V_2 > 1$, the direct ionization process is the dominant one and for $Z_1 \approx Z_2$ and $V_1/V_2 << 1$, electron capture process is predominant [1]. The cross sections by direct ionization process are calculated by ECPSSR theory [2] and RPWBA theory [3–6] derived from PWBA theory [7]. The ECPSSR theory includes correction for particle energy loss (E), Coulomb deflection of incident particle (C), polarization and binding energies of the electrons in perturbed stationary state (PSS) and relativistic effect (R). Based on ECPSSR theory, the K and L shell ionization cross sections were calculated and tabulated by Cohen and Harrigan [8]. Chen and Crasemann [9] have calculated the ionization cross section for proton impact relativistically (R) with Dirac-Hartree-Slater (DHS) wave functions, which include corrections for binding energy, polarization and Coulomb deflection (BC) [RPWBA-DHS-BC].

The measured K-shell ionization cross sections have been well explained theoretically. However, the L sub-shell ionization cross sections and the relative L X-ray intensities for some heavy elements calculated on the basis of ECPSSR theory show some discrepancies with the experimental values [10–16]. Cohen [17,18] tried to explain the discrepancy between experimental and theoretical L-shell cross sections in terms of Coulomb effects and found [19] that Coulomb deflection effects could not explain them. Cohen [20] remarked that the discrepancy in L-shell cross section may be reduced by choosing a proper combination of fluorescence yields, C–K transition yields and X-ray transition rates.

*Corresponding Author

To convert the ionization cross sections to production cross sections, an accurate knowledge of the fluorescence yields (ω_i), C–K transition yields (f_{ij}) and X-ray transition rates are needed. For the *K*-shell process, the fluorescence yield data of Krause [21] and the theoretical emission rates of Scofield [22] are considered to be the acceptable database. But the situation is not clear for *L* X-rays because of the lack of proper fluorescence yields and C-K transition yield data. In the case of *L* X-rays, it is not possible to suggest any one set of database, because of the non-availability of *L* X-ray cross sections in different regions of the periodic table. The experimental *K* and *L* sub-shell fluorescence yields and *L* shell C–K transition yields were compiled by Krause [21]. Cohen [20] suggested that the ω_i and f_{ij} values of Krause form a good database with the experimental transition rates of Salem *et al* [23]. Campbell [16] suggested that the cross section tabulations of Chen and Crasemann [6] together with the fluorescence yields, Coster-Kronig transitions of Chen *et al* [24], and the emission rates of Scofield [22] also form a self-consistent database.

The *L* X-ray production cross sections in Pb and Bi have been calculated theoretically by Xu and Xu [25] using ECPSSR and PRWBA-DHS-BC ionization cross sections with different sets of ω_i and f_{ij} values. They have calculated the ECPSSR ionization data using the fluorescence yield data of Xu and Xu [25] and fits well with the experimental data. Padhi *et al* [26] have measured the *L* X-ray production cross sections and their relative intensities in elements Pb and Bi using proton beam. Their results indicate that the measured relative intensities of Pb agree partly with the theoretical ratios obtained from ECPSSR ionization cross sections and decay yields data of Xu and Xu [25] and partly with the results obtained using Krause decay yields data. In the case of Bi, Padhi *et al* [26] have obtained good agreement with the RPWBA-DHS-BC results in the entire energy region. In the high energy region, their experimental values show good agreement with the cross sections of ECPSSR theory coupled with Krause decay yield data and in the low energy region, with the ECPSSR cross section data coupled with the decay yields of Xu and Xu [25]. Sow *et al* [27] measured the X-ray production cross sections in some medium *Z* elements with proton bombardment. Their *L* X-ray production cross section data show a reasonable agreement with the ECPSSR predictions. Their results indicate that the theoretical values obtained using the fluorescent yields and C–K data of Chen *et al* [24] give a better agreement.

The purpose of the present study is to measure the *L* X-ray intensity ratios (ratios of production cross sections) in elements Ta, W, Au, Pb and Bi with 2 MeV proton beam. The results thus obtained are compared with the theoretical intensity ratios calculated using ECPSSR and RPWBA-BC ionization cross sections along with different sets of decay yield data.

2. Experimental details

In the present work, proton beams of 2 MeV energy are used to excite the samples. The pelletron accelerator facility available at the Institute of Physics, Bhubaneswar is used for these measurements. Out of the six elements selected for measurement of *L* X-ray intensity ratios, the elements Ta, Au and Pb are prepared as thin foils. The other elements namely W, Hg and Bi are taken in the form of chemical compounds. The targets are kept vertically in the scattering chamber at an angle of 45° to the beam direction. A ladder arrangement is provided in the scattering chamber to keep four targets at a time and bring the required target into the beam position. An observation window is provided to the scattering chamber. By viewing through this window, the target is adjusted so that the proton beam falls centrally on the required target.

The *L* X-rays emitted from the target are detected using a high resolution Si(Li) detector. The detector is mounted at an angle of 90° to the beam direction. The resolution of the detector used in the present work is 160 eV FWHM at energy of 5.9 keV. The *L* X-ray spectrum of Ta, W, Au, Hg, Pb and Bi elements is recorded. The spectra are collected for sufficiently long time so as to get good statistical accuracy. The *L* X-ray spectrum of Tantalum obtained in the present work is shown in Figure 1. From the figure, it may be seen that the different *L* X-ray components L_l, L_α, L_β and L_γ are clearly separated.

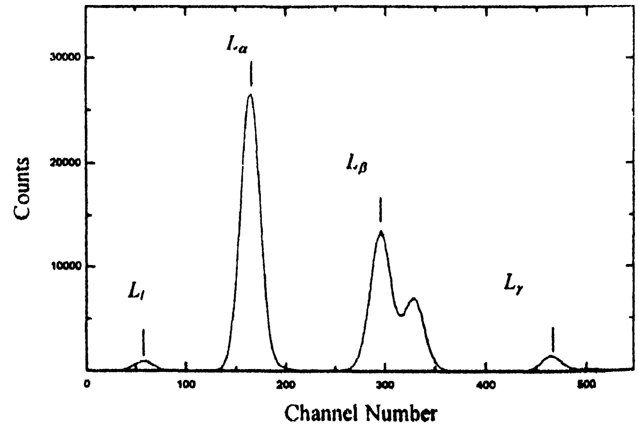

Figure 1. *L* X-ray spectrum of Tantalum with 2 MeV proton beam

3. Data analysis

When the projectile approaches close to the target nucleus, the influence of nuclear forces can no longer be neglected compared to the coulomb forces. The Rutherford cross section can not then predict the elastic scattering cross section [28,29]. Hence in the present work, instead of measuring the absolute L X-ray production cross sections, L X-ray intensity ratios are measured so that the parameters such as Rutherford scattering cross sections, back scattered particles yield and solid angle cancel out. Shafroth [30] has pointed out that from the experimental point of view, the measurement of L X-ray intensity ratios eliminate many uncertainties such as inhomogeneity of target thickness, uncertainties in the geometry measurement and the ion current. These L X-ray intensity ratios are the same as the ratio of the corresponding L X-ray production cross sections. Hence,

$$\frac{I_{\mathrm{Li}}}{I_{\mathrm{Lj}}} = \frac{\sigma_{\mathrm{Li}}}{\sigma_{\mathrm{Lj}}}. \tag{1}$$

From Figure 1, it may be seen that the L_l, L_α, L_β and L_γ X-ray components are clearly resolved. The areas under different L X-ray components are estimated. From the efficiency curve [31], the efficiency values corresponding to the energies of different L X-ray components are taken and used in converting the areas under different L X-ray components to their corresponding intensities. These intensities are corrected for self-absorption of the X-rays in the target material. The corresponding mass attenuation coefficients are taken from the tables of Storm and Israel [32]. Finally, the intensity ratios L_α/L_l, L_α/L_β and L_α/L_γ are evaluated for each element and the values thus obtained are given in Table 1.

Table 1. Experimental and theoretical L X-ray intensity ratios

Z/Ratio	Experimental		Theory	
	Present	Other data	RPWBA	ECPSSR
$_{73}$Ta				
L_α/L_l	21.24 ± 1.1	18.15[35], 21.58[36]	—	21.39(X), 21.67(Y)
L_α/L_β	1.81 ± 0.08	1.52[35], 1.85[36]	—	1.74(A), 1.78(B), 1.73(C), 1.77(D)
L_α/L_γ	13.62 ± 0.6	10.98[35], 14.03[36]	—	12.78(A), 13.66(B), 12.67(C), 13.33(C)
$_{74}$W				
L_α/L_l	20.90 ± 1.1	21.02[37](X), 21.36[37](Y)	21.02(X), 21.36(Y)	21.02(X), 21.36(Y)
L_α/L_β	1.68 ± 0.08	1.58[37](A), 1.61[37](B), 1.57[37](C), 1.62[37](D)	1.62(A), 1.66(B), 1.60(C), 1.68(D)	1.75(A), 1.81(B), 1.73(C), 1.78(D)
L_α/L_γ	11.76 ± 0.55	10.80[37](A), 11.56[37](B), 10.79[37](C), 11.57[37](D), 10.38[37](E), 11.59[37](F)	11.39(A), 12.21(B), 11.22(C), 12.00(D), 11.32(E), 11.11(F)	12.91(A), 13.82(B), 12.70(C), 13.59(D), 12.80(E), 13.70(F)
$_{79}$Au				
L_α/L_l	19.59 ± 1.1	19.82[38](X), 19.88[38](Y)	19.82(X), 19.88(Y)	19.82(X), 19.88(Y)
L_α/L_β	1.80 ± 0.09	1.77[40](A), 1.73[40](B), 1.56[40](C), 1.61[40](D), 1.77[39](A), 1.88[39](B), 1.67[39](C), 1.73[39](D)	1.77(A), 1.82(B), 1.64(C), 1.69(D)	1.93(A), 1.99(B), 1.77(C), 1.90(D)
L_α/L_β	13.63 ± 0.70	12.70[40](A), 13.33[40](B), 10.37[40](C), 11.98[40](D), 13.15[39](A), 16.40[39](B), 11.43[39](C), 13.12[39](D)	12.75(A), 14.23(B), 11.28(C), 13.02(D)	14.85(A), 17.18(B), 13.13(C), 15.18(D)
$_{80}$Hg				
L_α/L_l	19.42 ± 1.1	—	—	19.57(X), 21.07(Y)
L_α/L_β	1.86 ± 0.09	—	—	1.99(A), 2.22(B), 1.85(I)
L_α/L_γ	13.83 ± 0.7	—	—	15.13(A), 17.81(B), 14.25(I)
$_{82}$Pb				
L_α/L_l	18.52 ± 1.0	18.94[41](X), 18.97[41](Y)	—	18.94(X), 18.97(Y)
L_α/L_β	1.82 ± 0.09	1.72[41](A), 1.75[41](B), 1.61[41](G), 1.57[41](H)	—	1.98(A), 2.04(B), 1.79(G), 1.84(H)
		1.87[38](A), 1.92[38](B), 1.81[38](G), 1.71[38](H)		1.86(C), 1.91(D), 1.88(I)
L_α/L_γ	13.91 ± 0.7	11.89[41](A), 12.70[41](B), 10.88[41](G), 10.42[41](H), 13.72[38](A), 14.59[38](B), 12.18[38](C), 12.97[38](D)		15.56(A), 16.51(B), 12.88(G), 13.66(H), 13.71(C), 14.55(D), 14.49(I)

Table 1. *(Cont'd.)*

Z/Ratio	Experimental		Theory	
	Present	Other data	RPWBA	ECPSSR
$_{83}$Bi				
L_α/L_l	18.43 ± 1.0	18.66[41](X), 18.69[41](Y)	18 66(X), 18.69(Y)	18.66(X), 18.69(Y)
L_α/L_β	1.79 ± 0 09	1 75[41](A), 1 74[41](B), 1 69[41](E), 1.76[41](F), 1.65[41](G), 1.55[41](H)	1.74(A), 1.81(B), 1.74(E), 1.72(F), 1.69(G), 1.62(H)	1.91(A), 2.00(B), 1.92(E), 1.91(F) 1.80(G), 1.79(H), 1.89(I)
L_α/L_γ	13.48 ± 0.70	12 26[41](A), 13.09[41](B), 11.57[41](E), 13 25[41](F), 11 29[41](G), 10.69[41](H)	13.15(A), 13.97(B), 12.21(E), 14.12(F), 11.67(G), 11.47(H)	15 72(A), 16.70(B), 14.56(E), 15.46(F), 12.90(G), 13.70(H), 14.70(I)

X . Campbell and Wang [34] Y : Scofield (X-ray emission rates) [22]
A : (Krause-Campbell) [21,34] B · (Krause-Scofield) [21,22] C · (Werner-Campbell) [33,34] D : (Werner-Scofield) [33,22]
E . (Chen-Campbell) [24,34] F · (Chen-Scofield) [24,22] G · (Xu-Xu, Krause-Campbell) [25,21,34] H : (Xu-Xu, Krause-Scofield) [25,21,22]
I : (Krause-Salem) [21,29]

The present L X-ray intensity ratios are associated with an overall uncertainty of about 5%. This error is calculated by applying the method of propagation of individual errors due to counting statistics, efficiency correction and self-absorption correction.

4. Calculation of X-ray production cross section from ionization cross section

The L X-ray production cross sections are obtained from the ionization cross sections using the following relations [26] :

$$\sigma^X_{Ll} = (\sigma_{L1}f_{13} + \sigma_{L1}f_{12}f_{23} + \sigma_{L2}f_{23} + \sigma_{L3})\omega_3 F_{3l},$$

$$\sigma^X_{L\alpha} = (\sigma_{L1}f_{13} + \sigma_{L1}f_{12}f_{23} + \sigma_{L2}f_{23} + \sigma_{L3})\omega_3 F_{3\alpha}, \quad (2)$$

$$\sigma^X_{L\beta} = \sigma_{L1}\omega_1 F_{1\beta} + (\sigma_{L1}f_{12} + \sigma_{L2})\omega_2 F_{2\beta} + (\sigma_{L1}f_{13} + \sigma_{L1}f_{13}f_{23} + \sigma_{L2}f_{23} + \sigma_{L3})\omega_3 F_{3\beta},$$

$$\sigma^X_{L\gamma} = \sigma_{L1}\omega_1 F_{1\gamma} + (\sigma_{L1}f_{12} + \sigma_{L2})\omega_2 F_{2\gamma},$$

where $\sigma^X_{Ll}, \sigma^X_{L\alpha}, \sigma^X_{L\beta}$ and $\sigma^X_{L\gamma}$ are the X-ray production cross section of L_l, L_α, L_β and L_γ X-ray components respectively, σ_{L1}, σ_{L2} and σ_{L3} are the ionization cross sections of L_1, L_2 and L_3 sub-shells respectively. ω_1, ω_2 and ω_3 are the corresponding sub-shell fluorescence yields and f_{12}, f_{23} and f_{13} are the Coster-Kronig transition probabilities.

Here, F_{ny} represents τ_{ny}/τ_n. For example $F_{3\alpha} = \tau_{3\alpha}/\tau_3$ where τ_3 is the theoretical total radiative transition rate of the L_3 shell and $\tau_{3\alpha}$ is the sum of the radiative transition rates which contribute to the L_α lines associated with the hole filling in the L_3 sub-shell that is,

$\tau_{3\alpha} = \tau_3(M_4 - L_3) + \tau_3(M_5 - L_3)$ where $\tau_3(M_4 - L_3)$ is the radiative transition rate from the M_4 shell to the L_3 shell.

For elements Ta, W, Au, Hg, Pb and Bi, the theoretical intensity ratios L_α/L_l, L_α/L_β and L_α/L_γ are calculated from the ionization cross sections due to ECPSSR theory [8] and RPWBA theory [6] at 2 MeV proton energy. These intensity ratios are calculated using the above formula, together with different data bases [fluorescence yields 'ω_i', C–K transition yields 'f_{ij}' and emission rates 'τ']. The fluorescence yields data of Krause [21], Werner and Jitschin [33], Chen *et al* [24], Xu and Xu [25] and the C–K decay yields of Krause [21], Werner and Jitschin [33] and Chen *et al* [24] are taken. The X-ray emission rates are taken from the tables of Scofield [22] and Campbell and Wang [34]. The fluorescence yields and C–K transition yields data due to different authors used in the present calculations are shown in Table 2. The theoretical intensity ratios thus obtained due to combinations of different databases and different cross section values are given in Table 1.

5. Results and discussion

The L X-ray production cross section ratios L_α/L_l, L_α/L_β and L_α/L_γ obtained in the present work in Ta, W, Au, Hg, Pb and Bi due to 2 MeV proton bombardment are shown in Table 1 along with the experimental uncertainties. In the same table, the intensity ratios calculated from the experimental cross section values due to different authors are also given.

L_α/L_l intensity ratio :

The L_α/L_l intensity ratios are independent of ionization cross section values, fluorescence yield values and C–K transition yields. This ratio depends only on X-ray transition rates. These ratios for elements Ta, W, Au, Hg, Pb and Bi are calculated with the theoretical transition rates due to Scofield [22] as well as Campbell and Wang [34]. The L_α/L_l intensity ratios obtained in the present work for the above elements are compared with the theoretical ratios computed from

Table 2. Fluorescence yield and C-K decay yield data of different authors

Author	ω_1	ω_1	ω_1	f_{12}	f_{13}	f_{23}
Ta(73)						
Krause [21]	0.137	0.258	0.243	0.18	0.28	0.134
Werner and Jitschin [33]	0.128	0.243	0.222	0.104	0.339	0.111
W(74)						
Krause [21]	0.147	0.270	0.255	0.17	0.28	0.133
Werner and Jitschin [33]	0.130	0.274	0.245	0.102	0.325	0.106
Chen *et al* [24]	0.137	0.290	0.264	0.185	0.350	0.139
Au(79)						
Krause [21]	0.107	0.334	0.320	0.14	0.53	0.122
Werner and Jitschin [33]	0.137	0.364	0.207	0.047	0.582	0.101
Hg(80)						
Krause [21]	0.107	0.347	0.333	0.13	0.56	0.120
Chen *et al* [24]	0.082	0.368	0.320	0.069	0.705	0.127
Pb(82)						
Krause [21]	0.112	0.373	0.360	0.12	0.58	0.11
Werner and Jitschin [33]	0.145	0.408	0.346	0.040	0.661	0.091
Xu and Xu [25]	0.135	0.405	0.326	–	–	–
Bi(83)						
Krause [21]	0.117	0.387	0.373	0.11	0.58	0.113
Chen *et al* [24]	0.099	0.410	0.354	0.055	0.7	0.12
Xu and Xu [25]	0.138	0.428	0.340	–	–	–

Scofield and Campbell and Wang transitions rates and found reasonable agreement within experimental uncertainties. From the table, it is seen that the L_α/L_l intensity ratios due to Scofield and Campbell and Wang transition rates differ by less than 1%.

L_α/L_β intensity ratio :

The L_α/L_β intensity ratios are calculated using the experimental cross section values of some of the earlier authors [35–41] with different data bases. The L_α/L_β intensity ratios thus obtained due to earlier authors are compared with the intensity ratios obtained in the present work. It is found that the earlier experimental intensity ratios obtained with the data bases [Krause-Scofield] and [Krause-Campbell] are in good agreement with the present experimental intensity ratios within experimental uncertainties. The L_α/L_β intensity ratios are also calculated using the theoretical cross sections values due to PWBA as well as ECPSSR theories employing different data bases. The theoretical intensity ratios thus obtained are compared with the intensity ratios obtained in the present work. It is found that the theoretical intensity ratios due to RPWBA along with the databases [Krause-Scofield] and [Krause-Campbell] are in agreement within experimental uncertainties. On the other hand, the L_α/L_β intensity ratios due to the cross section values of ECPSSR theory along with data bases [Krause-Scofield] and [Krause-campbell] are slightly higher than the present experimental values.

L_α/L_γ intensity ratio :

The L_α/L_γ intensity ratios are also computed from the experimental L-shell ionization cross section due to some of the earlier authors [35–41] employing different data bases. These intensity ratios obtained with data bases [Krause-Scofield] and [Krause-Campbell] are in agreement with the present intensity ratios within experimental uncertainty limits. From the table, it is seen that the L_α/L_γ intensity ratios obtained with the theoretical cross section values of RPWBA along with the data bases of [Krause-Scofield] and [Krause-Campbell] and [Werner-Scofield] are in agreement with the present experimental values. On the other hand, the intensity ratios obtained due to ECPSSR cross section values along with the data bases [Werner-Campbell], [Xu, Xu, Krause-Scofield] show agreement with the present experimental intensity ratios.

It is important to note that the theoretical intensity ratios obtained from the theoretical ionization cross sections are associated with uncertainties, which arises due to the uncertainties in the experimental fluorescence yields and C–K transition yields. If the uncertainties in both experimental and theoretical intensity ratios are considered, agreement between the experimental intensity ratios and the theoretical intensity ratios due to any of the databases is observed.

In the present work, since the L X-ray intensity ratios are measured only at 2 MeV proton energy, it is not possible to study the variation of these ratios with proton energy. Many of the earlier authors reported the data in the graphical form and a critical comparison between the experimental and the theoretical values is not possible. In the present work, therefore, the experimental and theoretical intensity ratios are presented in the tabular form.

Multiple ionization causes the fluorescence yields to increase. The fluorescence yields of multiply ionized atoms may be calculated if the exact configuration of the electrons and the vacancies in the target atom is known. Ramachandra Rao *et al* [42] have estimated the K-fluorescence yields due to multiply ionized atoms by using heavy ions as projectiles. Study of multiple ionization effects on L X-rays is more difficult to analyze [43,44]. This is because the satellite peaks produced by the vacancies in M and N shells are closely spaced that even crystal spectrometer cannot resolve them completely.

For light ions, the effect of multiple ionization is negligible. Fortner *et al* [45] have calculated the L-shell fluorescence yields in copper for different M-shell vacancies using the method developed by McGuire [46]. They have concluded that the L-shell fluorescence yields may be affected from the single hole values only when more than five multiple vacancies in the M-shell are produced. This is possible only when heavy ions are used as projectiles. In the present work, since protons are used as projectiles, multiple ionization effects may be neglected. Hence, the use of single hole fluorescence yields values and C–K transitions rates to convert the theoretical L-shell ionization cross sections to production cross sections is justifiable.

5. Conclusion

The experimental L X-ray intensity ratios obtained in the present work in the elements Ta, W, Au, Hg, Pb and Bi are compared with the intensity ratios calculated by using the experimental L X-ray ionization cross sections due to earlier authors and also with the theoretical cross sections of PWBA and ECPSSR theories along with different sets of data bases : fluorescence yields, C–K decay yields and L X-ray emission rates. The following conclusions are arrived at :

1. The difference in the L_α/L_l intensity ratios which are calculated using the emission rates of Scofield [22] and of Campbell and Wang [34] is less than 1%.
2. For all the elements under study, the L_α/L_β and L_α/L_γ intensity ratios obtained in the present work are in agreement with the previous experimental intensity ratios, and the theoretical intensity ratios due to RPWBA and ECPSSR theories which are calculated using the data bases [Krause-Scofield] and [Krause-Campbell] within the experimental uncertainties. However, if the uncertainties in the theoretical intensity ratios are also considered, then there is agreement between the present experimental ratios and the theoretical ratios that are calculated with any of the databases.

Acknowledgments

One of the authors Dr. S Bhuloka Reddy acknowledges the financial support provided by the Inter University Consortium for DAE facilities, Calcutta, India. The authors express their sincere thanks to the authorities of the Institute of Physics, Bhubaneswar for their hospitality.

References

[1] G Lapicki and R Mehta *Phys. Rev.* **A34** 3813 (1986)
[2] W Brandt and G Lapicki *Phys. Rev.* **A23** 1717 (1981)
[3] L Sarkadi and T Mukoyama *J. Phys.* **B21** L255 (1981)
[4] T Mukoyama and L Sarkadi *Phys. Rev.* **A25** 1411 (1982)
[5] M H Chen, B Crasemann and H Mark *Phys. Rev.* **A26** 1243 (1982)
[6] M H Chen and B Crasemann *At. Data Nucl. Data Tables* 33 217 (1985)
[7] E Merzbacher and H W Lewis *Handbuch der Physik* **34** ed
[8] M Cohen and D D Harrigan *At. Data. Nucl. Tables* **33** 255 (1985)
[9] M H Chen and B Crasemann *At. Data. Nucl. Data* **41** 257 (1989)
[10] W Jitschin, A Kaschaba, R Hippler and H O Lutz *J. Phys.* B15 763 (1982)
[11] J Braziewicz, M Pajck, E Braziewiczand and J Ploskonka *J Phys* **B17** 3245 (1984)
[12] J Braziewicz, M Pajck, E Braziewiczand, J Ploskonka and G M Osetynski *Nucl. Instrum. Meth.* **B15** 585 (1980)
[13] M Vigilante, P Cuzzocrea, N Decesare, F Muroloilante, M Cuzzocrea, P Decesare, N Murolo, F Perillo and E Spadaccimi *Nucl. Instrum. Meth.* **B15** 576 (1986)
[14] T J Gray and N Malhi *Bull. Am. Phys. Soc.* **35** 1713 (1990)
[15] M Harrigan and D D Cohen *Nucl. Instrum. Meth.* **B31** 576 (1986)
[16] J L Campbell *Nucl. Instrum. Meth.* **B31** 518 (1988)
[17] D D Cohen *Nucl. Insturm. Meth.* **218** 795 (1983)
[18] D D Cohen *Nucl. Instrum. Meth.* **B3** 47 (1984)
[19] M Harrigan and D D Cohen *Nucl. Instrum. Meth.* **B15** 581 (1986)
[20] D D Cohen *Nucl. Instum. Meth.* **B49** 1 (1990)
[21] M O Krause *J. Phys. Chem. Ref. Data* **8** 307 (1979)
[22] J H Scofield *At. Data Nucl. Data Tables* **14** 121 (1974)
[23] S I Salem, S L Panossian and R A Krause *At. Data Nucl. Data Tables* **14** 91 (1981)

[24] M H Chen, B Crasemann and H Mark *Phys. Rev.* **A24** 177 (1981)

[25] J Q Xu and X J Xu *J. Phys.* **B25** 695 (1992)

[26] H C Padhi, C R Buniya, B B Dhal and S Misra *J. Phys.* **B27** 1105 (1994)

[27] C H Sow, I Orlic, Osipowrica and S M Tang *Nucl. Instrum. Meth.* **B85** 133 (1994)

[28] M R McNeir, Y C Yu, D L Weather, D K Marble, Z Zhao, J L Duggan, F D Mc Daniel and G Lapicki *J. Phys.* **B27** 5295 (1994)

[29] M Bozorian, M K Hubbard and M Nastasi *Nucl. Instrum. Meth.* **B51** 311 (1990)

[30] S M Shafroth, G A Bissinger and A W Waltner *Phys. Rev.* **A7** 566 (1973)

[31] G A V Ramanamurty, K Ramachandra Rao, Y Ramakrishna, P Venkateswarlu, K Bhaska Rao, P V Ramana Rao, S Venkata Rathnam, V Seshagiri Rao, G J Naga Raju and S Bhuloka Reddy *Pramana-J. Phys.* **56** 697 (2001)

[32] E Storm and H J Israel *Nucl. Data Tables* **A7** 565 (1970)

[33] U Werner and W Jitschin *Phys. Rev.* **A38** 4009 (1988)

[34] J L Campbell and J X Wang *At. Data Nucl. Data Tables* **43** 281 (1989)

[35] K Ishii, S Morita, H Tawara, H Kaji and T Shiokawa *Phys. Rev.* **A10** 774 (1974)

[36] J Braziewicz, M Pajck, E Braziewicz, J Ploskonka and G M Osetynski *J. Phys.* **B17** 1589 (1984)

[37] E L Bjustiniano, A A G Nader, N V deCastro Faria, C V Barros Leite and A GdePinho *Phys. Rev.* **A21** 73 (1980)

[38] D D Cohen *J. Phys.* **B13** 2953 (1980)

[39] R S Sokhi and D Crumpton *Nucl. Instrum. Meth.* **181** 5 (1981)

[40] I Sarkadi and T Mukoyama *J. Phys.* **B13** 2255 (1980)

[41] C V Barros Leite, N Vde Castro Faria and A G de Pinho *Phys. Rev.* **A15** 943 (1977)

[42] K Ramachandra Rao, Y Ramakrishna, P Venkateswarlu, G J Naga Raju, K Bhaskar Rao, V Seshagiri and Bhuloka Reddy *Indian J. Phys.* (communicated) (2001)

[43] D K Olsen, C F Moora and P Richard *Phys Rev.* **A7** 1244 (1936)

[44] P G Burkhalter, A R Knadson and D J Nagel *Phys. Rev.* **A7** 1936 (1973)

[45] R J Fortner, R C Der, T M Kavanagh and J D Garcia *J Phys.* **5** L73 (1972)

[46] E J McGuire *Phys Rev.* **A3** 1801 (1971)